

Non-Fermi-liquid behavior of $\text{YbCu}_{5-x}\text{Al}_x$

E. Bauer, R. Hauser, A. Galatanu, H. Michor, and G. Hilscher
Institut für Experimentalphysik, Technische Universität Wien, A-1040 Wien, Austria

J. Sereni, M. G. Berisso, and P. Pedrazzini
Centro Atomico Bariloche, 8400 San Carlos de Bariloche, Argentina

M. Galli and F. Marabelli
Istituto Nazionale Nazionale per la Fisica della Materia, Dipartimento di Fisica "Alessandro Volta," Università di Pavia, I-27100 Pavia, Italy

P. Bonville

CEA, CE Saclay, DRECAM, Service de Physique de l'Etat Condensé, F-91191 Gif-sur-Yvette, France

(Received 22 April 1998; revised manuscript received 27 October 1998)

A valency change in $\text{YbCu}_{5-x}\text{Al}_x$ from $\nu \approx 2.2$ ($x=0$) to $\nu=3$ ($x=2$) causes a magnetic instability near a critical concentration $x_{\text{cr}} \approx 1.5$. Alloys in the vicinity of x_{cr} exhibit typical non-Fermi-liquid properties like a negative logarithmic contribution to the specific heat or substantial deviations of the electrical resistivity from a T^2 behavior. Both pressure and alloying in this series bring about a strong reduction of the Kondo temperature T_K ; the crystal-field interaction and the interatomic exchange gain therefore importance and magnetic order becomes possible beyond x_{cr} . [S0163-1829(99)03825-4]

I. INTRODUCTION

In recent investigations we have shown that a Cu/Al substitution in YbCu_5 causes a crossover from an almost non-magnetic $4f^{14}$ state (YbCu_5) to the magnetic $4f^{13}$ state in YbCu_3Al_2 .^{1,2} This change in the ground-state configuration is accompanied by the onset of long-range magnetic order and by an increase of both the ordering temperature and the magnitude of the ordered moment.

Such an evolution of the magnetic behavior, driven by a change of the valence, is promising with respect to the appearance of a non-Fermi-liquid (NFL) behavior near to the critical concentration x_{cr} at which long-range magnetic order sets in. There, a quantum critical point shall exist,³ and magnetic correlations can be much higher in energy than $k_B T_{N,(C)}$. As a consequence, the Fermi-liquid (FL) model is insufficient to account for the physical behavior of such systems.⁴ Previously, we have shown² that the specific heat of $\text{YbCu}_{3.5}\text{Al}_{1.5}$ behaves logarithmically at low temperature, indicating substantial deviations from a FL behavior. This particular alloy is in the proximity of the onset of long-range magnetic order in this series, which was confirmed by elastic neutron scattering experiments for $x=1.75$ ($T_N \approx 1$ K, $\mu_{\text{ord}} \approx 1.2\mu_B$) and $x=2$ ($T_N \approx 2$ K, $\mu_{\text{ord}} \approx 2\mu_B$).² More recently, a study of the magnetic susceptibility and of the temperature-dependent Mössbauer spectra revealed magnetic order below about 0.25 and 0.55 K for $x=1.6$ and 1.7, respectively.⁵

Investigations of Yb systems, in general, provide the possibility to approach a magnetic instability point from the opposite side when compared to isomorphous Ce systems. In particular, it was shown that the binary compound CeCu_5 , which is isostructural to YbCu_5 , orders antiferromagnetically below 4 K.⁶ While a Cu/Al substitution in the former suppresses long-range magnetic order, it is responsible for the occurrence of a magnetically ordered ground state in the latter. Moreover, we note that in both cases a simple antiferro-

magnetic structure was deduced from elastic neutron scattering experiments.^{2,6} Another important aspect of Yb systems is the fact that pressure can drive such systems from a nonmagnetic to a magnetic state, while Ce systems behave usually mirrorlike due to the electron-hole symmetry between the Ce^{3+} and the Yb^{3+} ions.

The aim of the present paper is to investigate in some detail the low-temperature physical behavior of alloys in a certain range around $x \approx x_{\text{cr}}$ and to show that NFL properties may occur also in Yb systems.

II. EXPERIMENTAL DETAILS

Samples with concentrations near to x_{cr} ($x=1.2, 1.3, 1.4, 1.5, 1.6,$ and 1.7) have been prepared from stoichiometric amounts of elements using high frequency melting. To ensure phase purity and homogeneity, the ingots were remelted several times and subsequently annealed for 10 days at 750 °C. X-ray diffraction measurements were carried out applying CoK_α radiation. The x-ray pattern proved phase purity (hexagonal CaCu_5 structure, $P6/mmm$), and revealed a continuous increase of the lattice parameter a and a slight decrease of c ; hence the volume of the unit cell grows with increasing Al content (see Fig. 1).

The electrical resistivity and magnetoresistivity of bar-shaped samples were measured using a four-probe dc method in the temperature range from 300 mK to room temperature. A liquid pressure cell with a 4:1 methanol-ethanol mixture as pressure transmitter served to generate hydrostatic pressure up to about 15 kbar. The absolute value of the pressure was determined from the superconducting transition temperature of lead.⁷

A superconducting quantum interference device magnetometer served for the determination of the magnetization from 2 K up to 300 K in fields up to 6 T.

Specific-heat measurements on samples of about 2 g were performed at temperatures ranging from 1.5 up to 60 K by

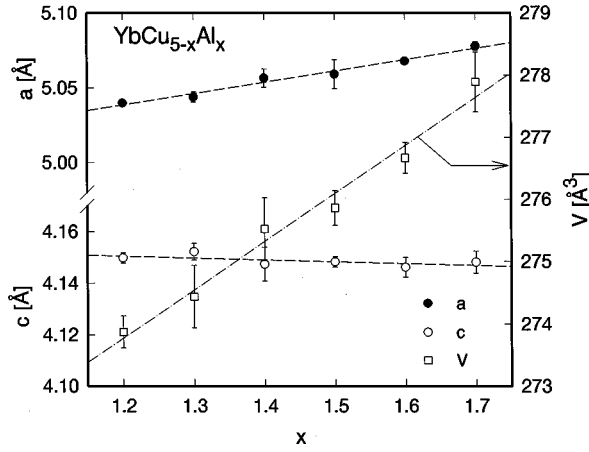


FIG. 1. Concentration-dependent variation of the lattice parameters a and c and of the volume V of $\text{YbCu}_{5-x}\text{Al}_x$ for various concentrations x .

means of a quasi adiabatic step-heating technique. Measurements down to 400 mK were carried out in a ^3He semiadiabatic calorimeter using the heat-pulse method and a three wires-Ge thermometry.

III. RESULTS

A. Physical properties at ambient conditions

1. Electrical resistivity

Figure 2 displays the temperature-dependent electrical resistivity $\rho(T)$ of $\text{YbCu}_{5-x}\text{Al}_x$ in a normalized representation for various concentrations x . The most prominent feature observed experimentally from the resistivity measurements is a concentration-dependent shift of a maximum in $\rho(T)$ at $T_{\rho,low}^{\max}$ from about 52 K for $x=1.3$ to about 0.9 K for $x=1.7$ (see inset, Fig. 2). No maximum in $\rho(T)$ was found in the available temperature range ($300 \text{ mK} < T < 300 \text{ K}$) and at ambient conditions for the alloy with $x=1.2$.

The overall shape of $\rho(T)$ for samples $x \leq 1.5$ is reminiscent of the behavior of a Kondo lattice, with a maximum at

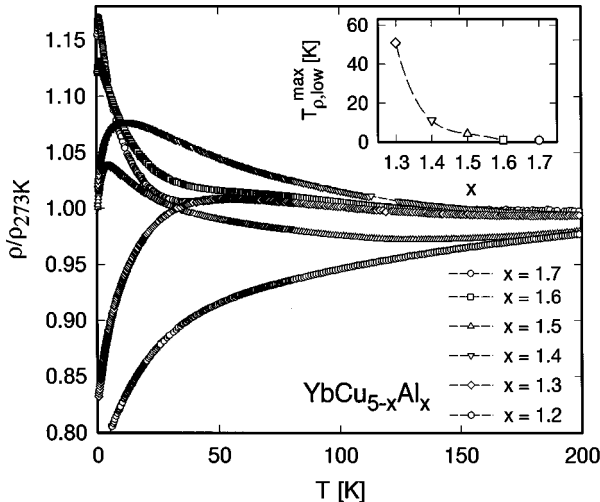


FIG. 2. Temperature-dependent electrical resistivity ρ of $\text{YbCu}_{5-x}\text{Al}_x$ for various concentrations x . The inset shows the concentration-dependent variation of $T_{\rho,low}^{\max}$.

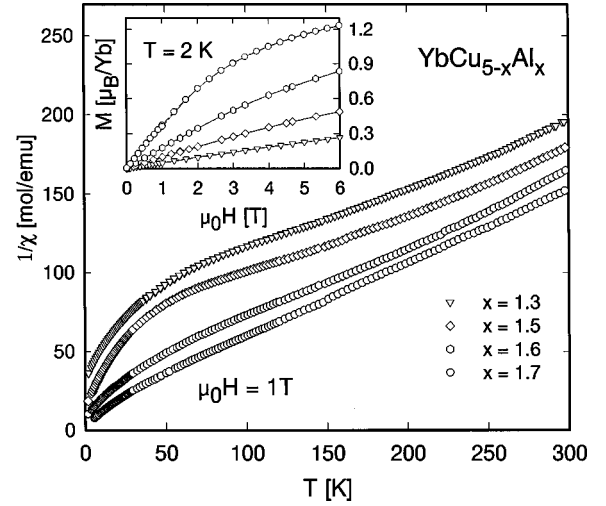


FIG. 3. Temperature-dependent inverse susceptibility $1/\chi$ of $\text{YbCu}_{5-x}\text{Al}_x$ for various concentrations x . The inset shows isothermal magnetization curves taken at $T=2 \text{ K}$.

$T_{\rho,low}^{\max} \propto T_K$,⁸ where T_K is the Kondo temperature of the lattice system. In the scope of this model, the Kondo interaction strength of the present series decreases along with growing values of x . The lowering of T_K causes a growing importance of the crystal-field (CF) interaction, since T_K may become much smaller than the energy of the first excited CF level. Previous ^{170}Yb Mössbauer studies on YbCu_3Al_2 revealed that the energy splitting between the first excited doublet and the ground-state doublet is about 100 K.¹⁰ In fact, this CF influence on the $\rho(T)$ behavior for $x=1.6$ and $x=1.7$ can be deduced from a shoulder centered around $T \approx 70 \text{ K}$. Below and above this shoulder, $\rho(T)$ can be accounted for in terms of the Kondo interaction in the CF ground state and in the excited CF level(s), respectively, together with an appropriate phonon contribution.⁹ A similar behavior occurs for $x=1.5$, the shoulder in $\rho(T)$ being however less pronounced. For smaller concentrations of Al, the CF influence cannot be resolved anymore from the $\rho(T)$ data. Additionally to the CF splitting, the decrease of T_K with growing Al content causes that the exchange interaction T_{RKKY} gains importance as evidenced from the onset of long-range magnetic order for $x \geq 1.6$ (with, however, reduced spontaneous magnetic moments).

2. Magnetic susceptibility

Magnetization measurements on various samples of this series have been performed from 2 K up to room temperature and at fields up to 6 T. The magnetization in the paramagnetic temperature range scales well with the applied field. Data taken at 1 T are shown in Fig. 3. The magnetic susceptibility $\chi(T)$ above about 50 K is characterized by a Curie-Weiss-like behavior and can be accounted for in a first approximation by $\chi(T) = \chi_0 + C/(T - \theta_p)$, with χ_0 being a temperature-independent Pauli susceptibility contribution, C is the Curie constant, and θ_p is the paramagnetic Curie temperature. The results of least-squares fits indicate that θ_p increases substantially from about -190 K for $\text{YbCu}_{3.7}\text{Al}_{1.3}$ to about -30 K for $\text{YbCu}_{3.3}\text{Al}_{1.7}$, while the effective magnetic moment μ_{eff} per Yb^{3+} ion, evaluated from the Curie con-

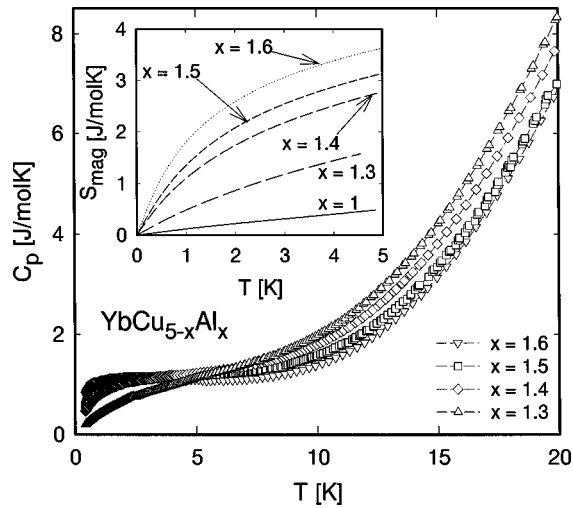


FIG. 4. Temperature-dependent specific heat C_p of various $\text{YbCu}_{5-x}\text{Al}_x$ alloys. The inset shows the temperature-dependent magnetic entropy S_{mag} in the low-temperature range.

stant, changes slightly from $4.49\mu_B$ for $x=1.3$ to $4.16\mu_B$ for $x=1.7$. The concentration dependent variation of θ_p may be understood as a decrease of T_K [$T_K \propto |\theta_p|$] (Ref. 11)] when the Al content rises. It is supposed that the decrease of μ_{eff} with growing Al content results from the crystal-field splitting, which changes slightly upon Al/Cu substitution.

The isothermal magnetization of $\text{YbCu}_{5-x}\text{Al}_x$ at 2 K, shown as inset in Fig. 3, significantly grows with increasing Al content and reflects the stabilization of the magnetic $4f^{13}$ state due to the Al/Cu substitution. This experimental finding is well in agreement with the evolution of the valence of the Yb ion as it was already demonstrated by means of L_{III} absorption edge spectroscopy.²

3. Specific heat

Specific heat measurements for $x=1.3, 1.4, 1.5,$ and 1.6 have been performed from 400 mK to about 100 K. Results of this study are shown in Fig. 4. The heat capacity C_p at low temperature ($T < 3$ K) increases with increasing Al content. However, at a temperature slightly above, a mirrorlike behavior is obtained, inferring that entropy is transferred from low to high temperature upon a lowering of the Al content. The inset of this figure shows the magnetic entropy S_{mag} calculated from the specific-heat data at low temperatures. Here, it should be mentioned that no “nonmagnetic” reference, yielding the phononic contribution C_{ph} could be subtracted as the appropriate series starting with LuCu_5 crystallizes in the cubic AuBe_5 -type structure.¹² However, since for the very low-temperature range $C_{\text{mag}} \gg C_{\text{ph}}$, we assume that $S \approx S_{\text{mag}}$. It is obvious from the inset of Fig. 4 that $S_{\text{mag}}(T)$ grows with increasing Al content. In terms of the Kondo effect, responsible for the release of entropy at low temperatures, the increase of S_{mag} with rising Al concentration indicates that the characteristic temperature of the system T_K decreases, in agreement with the resistivity and susceptibility results. The smooth behavior of $C_p(T)$ around $T=2$ K, with only a tiny anomaly for $x=1.3$ shows that the present samples are almost free from Yb_2O_3 .

In order to emphasize the electronic contribution to the specific heat at low temperatures, we have plotted C_p/T vs

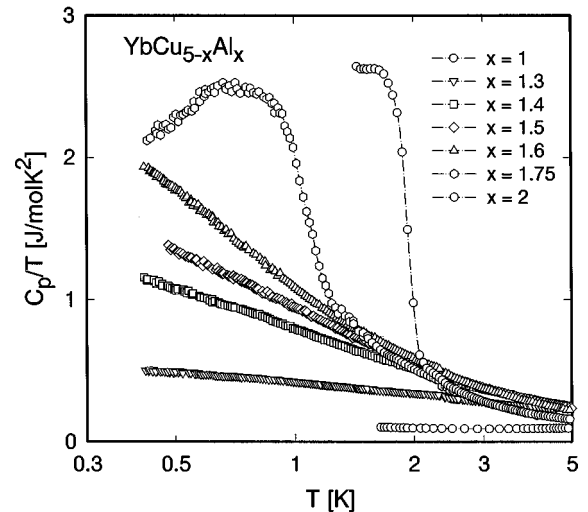


FIG. 5. Specific heat C_p of various $\text{YbCu}_{5-x}\text{Al}_x$ alloys plotted as C_p/T on a logarithmic temperature scale.

$\ln T$ of $\text{YbCu}_{5-x}\text{Al}_x$ in Fig. 5. The rise of the Al content causes at low temperature C_p/T to increase up to about 2 J/mol K^2 . This order of magnitude is typically observed for heavy fermion systems. Even for those alloys which are already magnetically ordered ($x \geq 1.6$), C_p/T remains very large. For Al concentrations slightly below the critical value ($1.3 \leq x \leq 1.5$), C_p/T behaves almost logarithmically below about 3 K. However, the sample with $x=1.3$ exhibits already a negative curvature at low temperatures. Finally, the alloy with $x=1$ shows just a weak temperature dependence, characteristic for an intermediate valence system and $C_p/T(T \rightarrow 0)$ can be extrapolated to about 100 mJ/mol K^2 . The most important feature of the heat capacity, however, is the logarithmic behavior, which is considered as a characteristic of a non-Fermi-liquid (NFL). Obviously, the observed $-\ln T$ dependence of C_p/T is related to the proximity of a magnetic instability owing to the Al/Cu substitution.

A similar evolution of the physical properties, in particular of the specific heat, has been observed in $\text{CeCu}_{6-x}\text{Au}_x$.¹³ In that case, the decrease of the Kondo coupling is assigned to an increase of the unit cell volume by the Cu/Au substitution. At the critical concentration for the onset of long-range magnetic order ($x_{\text{cr}} \approx 0.1$), significant deviations from the usual Fermi-liquid properties are observed.

B. Pressure and field-dependent properties of $\text{YbCu}_{5-x}\text{Al}_x$

1. Pressure response

In Figs. 6(a) and 6(b) the pressure dependence of the electrical resistivity is shown for $x=1.3$ and $x=1.6$, respectively, as an example of this series in the temperature range from 1.5 K up to 300 K and for pressures up to 12 kbar. As already mentioned, $\rho(T)$ of $\text{YbCu}_{3.7}\text{Al}_{1.3}$ exhibits at ambient pressure a maximum at $T_{\rho, \text{low}}^{\text{max}} \approx 52$ K while that of $\text{YbCu}_{3.4}\text{Al}_{1.6}$ occurs at 1.1 K. Upon an increase of pressure, $T_{\rho, \text{low}}^{\text{max}}$ of the former lowers; eventually reaching a value of about 9 K for $p=12$ kbar [compare Fig. 6(a)]. As can be inferred from the inset of Fig. 6(a), a pressure of the order of 25 to 30 kbar is sufficient to suppress $T_{\rho, \text{low}}^{\text{max}}$ below 1.5 K.

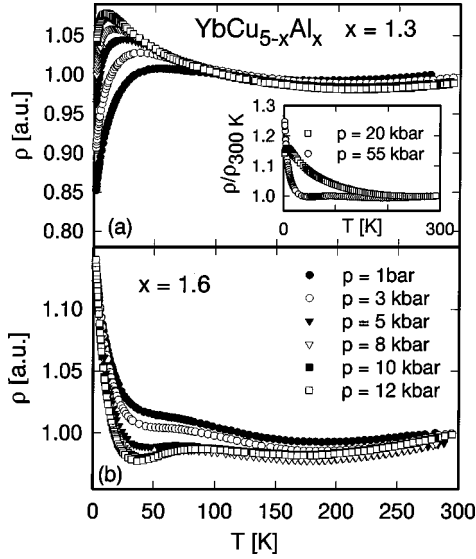


FIG. 6. Temperature and pressure-dependent electrical resistivity ρ of $\text{YbCu}_{3.4}\text{Al}_{1.6}$ and of $\text{YbCu}_{3.7}\text{Al}_{1.3}$.

Well above $T_{\rho,low}^{max}$ the resistivity behaves logarithmically due to the presence of Kondo interactions.

A growing value of the Al content x is accompanied by a decrease of $T_{\rho,low}^{max}$ (see inset, Fig. 2) and as a consequence, the value of the pressure sufficient to shift $T_{\rho,low}^{max}$ below 1.5 K decreases (e.g., $x = 1.4$: $p_{crit} \approx 10$ kbar). In the temperature range of the experiment, no pressure dependence of $T_{\rho,low}^{max}$ could be deduced for $\text{YbCu}_{3.4}\text{Al}_{1.6}$ [compare Fig. 6(b)].

The pressure-dependent decrease of $T_{\rho,low}^{max}$ indicates that T_K lowers, which is considered as a general feature of Yb systems.¹⁴ Such a behavior is opposite to Ce systems and is assumed to emerge from the electron-hole symmetry of both elements.

As the Al content grows, a second feature in $\rho(T)$ slightly below 100 K becomes evident due to CF splitting [compare Fig. 6(b)]. The resulting local maximum is further enhanced with rising values of pressure and the value of this temperature $T_{\rho,high}^{max}$ shifts moderately to higher temperatures. Even for $\text{YbCu}_{3.7}\text{Al}_{1.3}$ a local maximum at about 80 K appears due to the crystal-field splitting, however, at substantially enhanced values of pressure [$p > 30$ kbar, see inset, Fig. 6(a)], which is resolved when hybridization is sufficiently depleted. Logarithmic resistivity contributions are found at temperatures below and above those local maxima at $T_{\rho,high}^{max}$. In the scope of the model of Cornut and Coqblin,⁹ such a particular behavior follows from Kondo-type interactions in the presence of strong crystal-field splitting. The negative logarithmic resistivity behavior below and above $T_{\rho,high}^{max}$ reflects the Kondo effect in the crystal-field ground state and in an excited level, respectively, while the temperature of the maximum itself is a rough measure for the separation of the excited level from the ground state.

2. Field dependence

The field response of the alloys in the proximity of the critical concentration $x_{cr} \approx 1.5$ has been studied by means of electrical resistivity measurements up to 12 T and in a temperature range down to 300 mK.

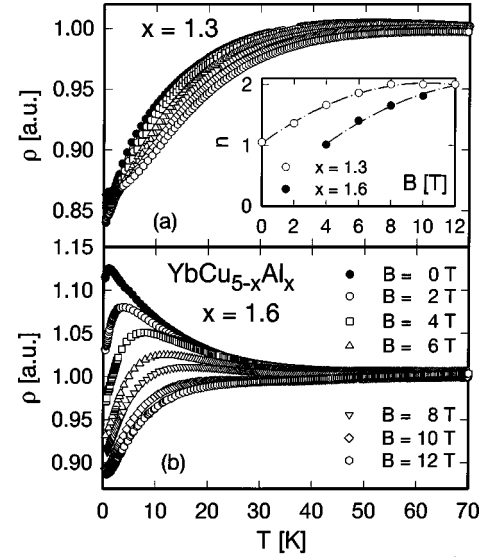


FIG. 7. Temperature and field-dependent electrical resistivity ρ of $\text{YbCu}_{3.4}\text{Al}_{1.6}$ and of $\text{YbCu}_{3.7}\text{Al}_{1.3}$.

As an example of our $\rho(T)$ results, measurements at constant fields as well as at constant temperatures are shown in Figs. 7, 8, and 9. While the alloy with $x = 1.2$ is characterized by a field induced increase of the resistivity in the temperature range $0.3 \leq T \leq 100$ K, the sample with $x = 1.3$ [Fig. 7(a)] reflects the case where the magnetoresistance is positive at low temperature, but crosses over to a negative one for a temperature above about 4 K. For concentrations $x > 1.3$, a negative magnetoresistance is observed for all fields in the temperature range covered [see Fig. 7(b)]. The maximum of $\rho(T)$ at $T_{\rho,low}^{max}$ becomes broader as the magnetic field grows and shifts to substantially higher temperature.

At lowest temperatures, the data was analyzed in terms of $\rho(T) = \rho_0 + AT^n$ (by taking the temperature range from 300 mK to 3 K, if possible). A T^2 behavior of the electrical resistivity, and thus a Fermi-liquid state, can be expected for Kondo lattices below the coherence temperature T_{coh} with $T_{coh} \ll T_K$. Kaga *et al.*^{15,16} pointed out that $T_{coh} \approx 0.1T_K$ in absence of any other interaction mechanisms. The exponent n for all the samples investigated is found to be strongly field dependent and increases, e.g., for $x = 1.3$ from about $n \approx 1$ at $\mu_0 H = 0$ T to $n = 2$ for fields roughly above 6 T [compare inset, Fig. 7(a)]. Along with the rise of the Al content, the saturation of the exponent n at a value of 2 occurs subsequently at higher fields. The deduced increase of n upon increasing external fields and the off-leveling at a value of $n = 2$ indicates that a Fermi-liquid state for the Cu-rich alloys is recovered in the presence of sufficiently strong magnetic fields.

As for the other samples, the field increase causes a rise of the exponent n for $x = 1.7$; however, even at $\mu_0 H = 12$ T a T^2 behavior is not recovered. This is either due to a limited access to low temperatures or, in our opinion, due to short-range order correlations above a magnetic phase transition, which cannot be quenched even in fields of 12 T.

In a simple view on Kondo systems one would expect that the decrease of T_K , driven by the Al substitution, should cause that already relatively lower fields are sufficient to quench Kondo-like spin fluctuations and restore Fermi-liquid

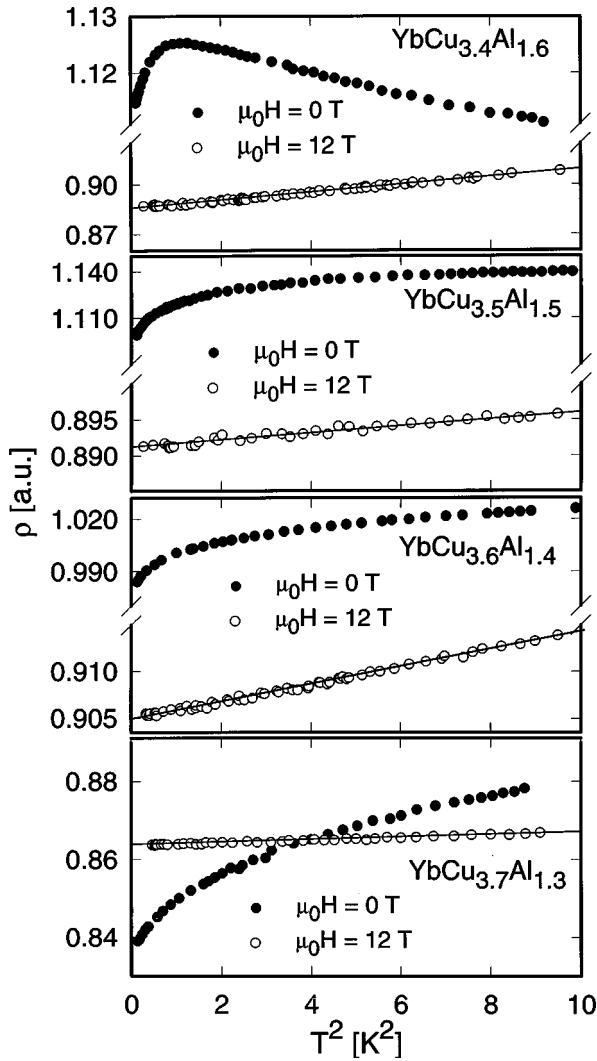


FIG. 8. Low temperature and field-dependent electrical resistivity ρ of $\text{YbCu}_{5-x}\text{Al}_x$ for $x=1.3, 1.4, 1.5,$ and 1.6 .

properties. Such a straightforward behavior, however, is expected to be valid only for systems with $T_K > T_{\text{RKKY}}$. Since with growing Al content $T_K \sim T_{\text{RKKY}}$ and eventually $T_K < T_{\text{RKKY}}$, the field response of the alloys investigated cannot longer be attributed to the Kondo effect only; rather the combined interaction of both processes apparently cause a different response of the system to magnetic fields and the locking of the exponent n at a value of 2 occurs in much larger fields than expected from the reduced values of T_K .

The magnetic phase transition temperature of $\text{YbCu}_{3.3}\text{Al}_{1.7}$ with $T_N \approx 0.55$ K and an estimated moment $\mu_{\text{ord}} \approx 0.6 \mu_B$ would imply that fields of the order of 1 T ($k_B T_N = g \mu_{\text{ord}} H$, g is assumed to be 2) should be sufficient to quench magnetic order, in contradiction to the experimental results. A possible explanation for such a discrepancy may be found from the fact that the strength of magnetic interactions is likely better described by the energy scale $k_B T_{\text{RKKY}}$, which in systems with a Kondo contribution may be substantially different from the deduced transition temperature.¹⁷ For $\text{YbCu}_{3.3}\text{Al}_{1.7}$, T_{RKKY} was calculated to be 5.7 K,⁵ which is about one order of magnitude larger than the value of T_N . Nevertheless, alloys and compounds with small ordering temperatures may represent examples where the Kondo cou-

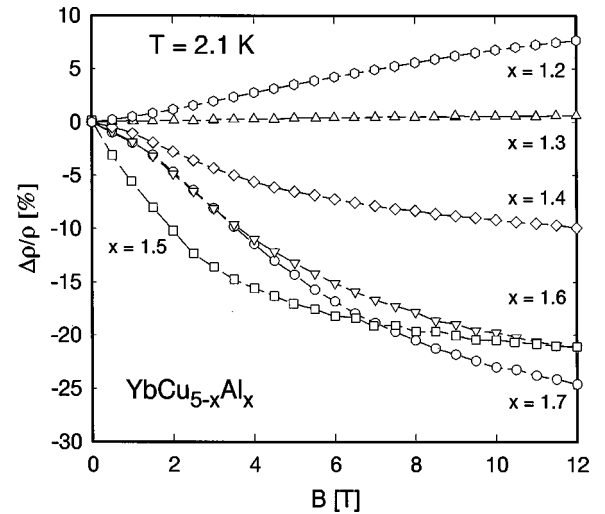


FIG. 9. Magnetoresistance $\Delta\rho/\rho$ of $\text{YbCu}_{5-x}\text{Al}_x$ for various concentrations x at $T=2$ K.

pling, the exchange interaction and the externally applied magnetic field can yield extraordinary complex interferences.

The field dependence of the low temperature resistivity for alloys with $1.3 \leq x \leq 1.6$ is shown in Fig. 8 plotted on a quadratic temperature scale. Obviously, common to all alloys is the nonquadratic temperature dependence of $\rho(T)$ at zero fields, while the 12 T measurement clearly displays a T^2 behavior from about 300 mK to 3 K. As already mentioned, enhanced spin fluctuations for the alloys in the proximity of the magnetic instability may be responsible for the observed deviations from the Fermi-liquid behavior; sufficiently strong fields, however, recover the FL state.

To show in more detail the characteristic crossover from a positive magnetoresistance to a negative one when increasing the Al content, $\Delta\rho/\rho$ is plotted in Fig. 9 for $1.2 \leq x \leq 1.7$ at $T=2.1$ K up to 12 T. At this temperature the alloy with $x=1.2$ shows large positive values and $x=1.3$ exhibits only a tiny positive magnetoresistance (about 0.8% at 12 T), while for $x=1.4$ the magnetoresistance is already negative (about 10% at 12 T) and increases to about 25% for $x=1.7$. It is interesting to note that $\Delta\rho/\rho$ for $x=1.5$ does not follow the continuous trend of the other concentrations. The magnetoresistance of this alloy initially decreases strongly with increasing field, but saturates for external fields above 6 T.

In terms of the Kondo-type interaction present in this series, the overall behavior may follow from an evolution of the ground-state behavior. While a positive magnetoresistance is usually found for coherent ground states, a negative magnetoresistance is related to interactions of conduction electrons with isolated Kondo scattering centers.

IV. DISCUSSION

The experimentally observed evolution of the physical properties in $\text{YbCu}_{5-x}\text{Al}_x$ appears to be primarily a result of a valence change either due to the Cu/Al substitution or due to pressure. This valence change is accompanied by a significant decrease of T_K . As a consequence, intersite interactions of the Ruderman-Kittel-Kasuya-Yosida (RKKY) type between the Yb ions gain weight and eventually, beyond a critical Al concentration x_{cr} , the system is expected to exhibit

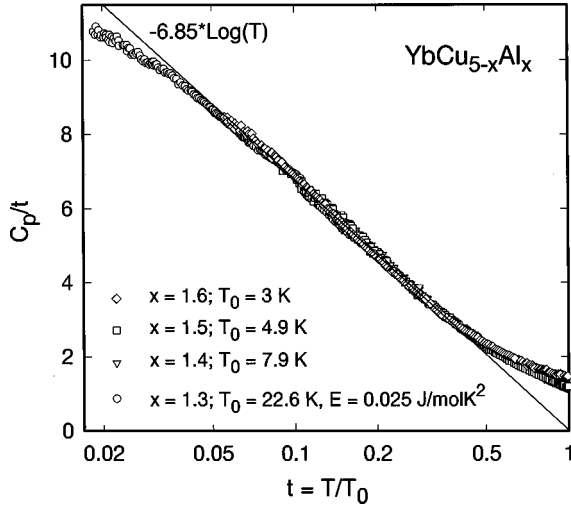


FIG. 10. Scaling of the “log t ” dependence of various $\text{YbCu}_{5-x}\text{Al}_x$ alloys.

a magnetic instability at $T \approx 0$. Such a zero-temperature phase transition influences observable physical properties even at finite temperatures.^{18–20} Most prominent is a negative logarithmic contribution to the specific heat and deviations of the electrical resistivity from the T^2 behavior. Experimentally, significant differences to a Fermi-liquid behavior were found for Al concentrations near to $x_{\text{cr}} \approx 1.5$. There, a critical balance of T_K and T_{RKKY} gives rise to a magnetic instability. The lowering of T_K is also responsible for a ground-state change in $\text{YbCu}_{5-x}\text{Al}_x$. While for smaller Al concentrations T_K is much larger than both RKKY and crystal-field splitting, the growing Al content reverses the former relation and crystal-field splitting as well as long-range magnetic order may dominate the physical properties.

In the scope of a phenomenological systematics²¹ it has been shown that the temperature dependence of the heat capacity of non-Fermi-liquid systems follows a general scaling law:

$$C_p/t = -D \log t + ET_0, \quad (1)$$

where $t = T/T_0$ and T_0 is the characteristic temperature of the system ($T_0 \sim T_K$). The constant D was deduced for most of the cerium based non-Fermi liquids as $D = 7.2 \text{ J/mol K}$ and $0 \leq E \leq 0.14 \text{ J/mol K}^2$.²¹ In order to check that scaling also for the Yb series investigated, we have plotted our low-temperature data in the normalized representation C_p/t vs $\log t$. Results are shown in Fig. 10. A scaling behavior with reasonable agreement is found from the procedure according to Eq. (1) for $x = 1.3, 1.4, 1.5$, and 1.6 with characteristic temperatures $T_0 = 22.6, 8, 5$, and 3 K , respectively. For concentrations between $x = 1.6$ and $x = 1.4$, T_0 increases slightly, while $E \approx 0$. However, for $x = 1.3$ both T_0 and E grow substantially; this behavior coincides with the approach of the unstable valent regime. The coefficient D is deduced for this series as $D = 6.85 \text{ J/mol K}$, thus being slightly smaller than the generally used value for cerium systems. The magnetic entropy associated with an idealized behavior according to the slope D and for temperatures from 0 to $t = 1$ follows from $\int_0^1 C_p/t dt = -\int_0^1 D \log t dt = 0.434D$. The entropy release up to the characteristic temperature T_0 amounts, therefore,

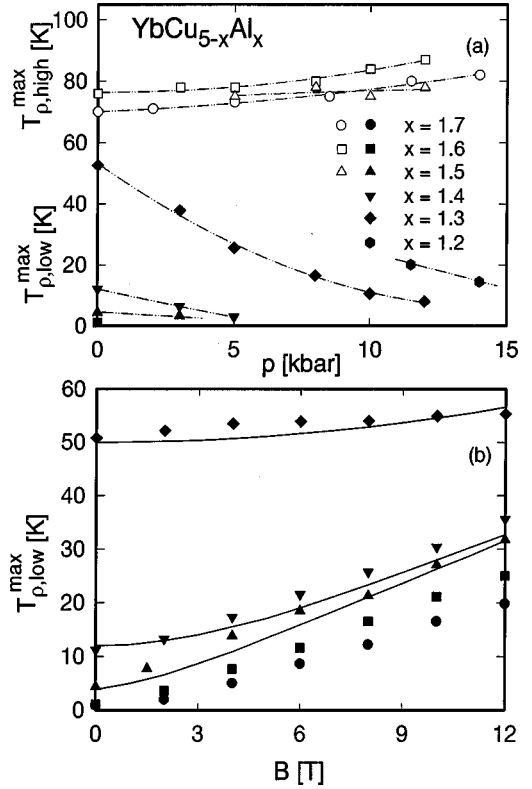


FIG. 11. Pressure (a) and field (b) dependence of characteristic temperatures of $\text{YbCu}_{5-x}\text{Al}_x$. The solid lines in (b) refer to variational calculation described in detail in the text.

roughly to $0.5R \ln 2$. For temperatures $t < 0.05$, C_p/T deviates from the expected logarithmic behavior. Thus, the entropy derived from the experiment is slightly less than calculated from Eq. (1). Both from the theoretical and the experimental point of view,^{4,22,23} the low temperature limit of the specific heat at a quantum critical point should behave like $\gamma = \gamma_0 - \alpha T^{1/2}$. Such a dependence would provide a natural explanation for the observed low-temperature data of the Yb series studied. However, an experimental study well below 400 mK is necessary in order to draw a final conclusion. For $x = 1.3$, the finite value of E_0 causes an additional contribution to S_{mag} , amounting to $0.56 \text{ J/mol K} \approx 0.1R \ln 2$ at $t = 1$. Though C_p/t does not become zero at $t = 1$, the remnant entropy above that temperature is far from reaching the expected value of $R \ln 2$.²⁴

The influence of substitution and pressure on the characteristic temperatures of the system was deduced from distinct features like maxima or weak local maxima of the temperature dependent resistivity. Results are plotted in Fig. 11. Two different physical mechanisms cause such maxima in $\rho(T)$: i) For $x \geq 1.5$ the crystal-field splitting in the presence of a Kondo interaction is responsible for the high-temperature maximum $T_{\rho,high}^{\text{max}}$ showing only a small concentration dependence. Pressure shifts this resistivity maximum to higher temperatures. This can be explained in terms of the simple point-charge model, where, putting the ionic charges closer together, the increasing Coulomb potential enlarges the overall crystal-field splitting. (ii) It is obvious from Fig. 2 that the alloys with smaller Al content do not exhibit evidence of crystal-field effects. These samples are characterized by a maximum at $T_{\rho,low}^{\text{max}}$ (for $p = 1 \text{ bar}$) which increases in tem-

perature when the Al content is further reduced. $T_{\rho,low}^{\max}$ is, in absence of any additional interaction mechanisms, a measure of the Kondo temperature T_K .⁸ Intersite interactions of the RKKY type can modify this relation. Pethick and Pines²⁵ showed that in such a case the low-temperature physics is governed by a new temperature scale T^* according to

$$T^* = T_K [1 - CJ(q,0,T)/T_K], \quad (2)$$

where C is the Curie constant and $J(q,0,T)$ is the wave vector-dependent-intersite coupling constant at zero frequency and at a temperature T . Equation (2) indicates that for $T_K > CJ(q,0,T)$, the characteristic temperature T^* coincides essentially with the Kondo temperature T_K , while in the opposite case, i.e., $T_K < CJ(q,0,T)$, RKKY interactions dominate T^* .

The concentration-dependent decrease of $T_{\rho,low}^{\max}$ is depicted in the inset of Fig. 2. Obviously, $T_{\rho,low}^{\max}$ changes in a nonlinear way with x and becomes almost concentration independent for $x \geq 1.6$. In terms of Eq. (2), $T_{\rho,low}^{\max}(x)$ reflects the crossover from the Kondo dominated concentration range (small values of x) to the range where RKKY interaction becomes comparable to, or even exceeds the Kondo energy. In fact, the alloy with $x = 1.6$ is found to exhibit long-range magnetic order below about 250 mK Ref. 10 and T_N increases with further increasing x .

A similar behavior follows also from the pressure response of $T_{\rho,low}^{\max}$. Increasing values of pressure cause, as already discussed, a decrease of $T_{\rho,low}^{\max}$. However, $dT_{\rho,low}^{\max}/dp$ is strongly concentration dependent and the initial value of $dT_{\rho,low}^{\max}/dp$ lowers with growing Al substitution from e.g., -5.4 K/kbar for $x = 1.3$ to -0.4 K/kbar for $x = 1.5$. Moreover, as follows most clearly from the alloy with $x = 1.3$, $dT_{\rho,low}^{\max}/dp$ decreases upon rising values of pressure. This behavior is likely also a consequence of Eq. (2), since, as it is well known, the pressure response of T_K is large. Thus, as T_K is significantly lowered by pressure in a particular system, the RKKY interaction becomes of comparable magnitude and finally surpasses T_K . For a system where the RKKY interaction dominates over T_K , much smaller values of $dT_{\rho,low}^{\max}/dp$ may be expected.¹⁴

Both the concentration- and the pressure-dependent reduction of T_K have to be originated from different physical mechanisms. On the one side this follows from an increase of the unit-cell volume due to the Al/Cu substitution (equivalent to a negative chemical pressure), while on the other side hydrostatic pressure shrinks the volume of the unit cell. However, as both effects are opposite, we have to conclude that the former follows primarily from electronic effects due to the substitution of a monovalent element (Cu) by a trivalent one (Al). The optical conductivity $\sigma(\omega)$ of this series²⁶ indicates a tendency towards a decrease of the number of free carriers upon an increasing Al content. As a consequence, the electronic density of states at the Fermi energy, $N(E_F)$, is expected to decrease, too. The latter does not contrast the observed increase of the low-temperature C_p/T values. Actually, the free carrier density evaluated from $\sigma(\omega)$ refers to an extended energy range (up to 2 eV) and can thus be associated with the high-temperature metallic properties of the alloys. The interaction of the $4f$ states with the con-

duction electrons, and the renormalization of the density of states, however, occurs at a much lower energy scale which is of the order of the Kondo temperature T_K .

Defining T_K in the usual way by $T_K \propto \exp[-1/(J_{kf}N(E_F))]$ and taking into account the Schrieffer-Wolff transformation for the coupling constant J_{kf} as $J_{kf} = |V_{kf}|^2/|\epsilon_f|$ (V_{kf} is the hybridization matrix element between the f and the conduction electron states and ϵ_f is the energy of the $4f$ level with respect to the Fermi energy E_F), yields the following conclusions: A lowering of T_K may be referred to a decrease of $N(E_F)$ and/or to a reduction of $|V_{kf}|^2/|\epsilon_f|$. Since the Yb ion approaches the $3+$ configuration on the Al increase, the $4f$ state becomes more localized. Therefore, $|V_{kf}|$ is thought to decrease as well. To a first approximation, the reduction of both quantities $N(E_F)$ and $|V_{kf}|$ explains the observed decrease of T_K in $\text{YbCu}_{5-x}\text{Al}_x$ upon the rising Al content.

The pressure-dependent reduction of T_K as a function of increasing pressure may be understood from the fact that the number of f holes n_f in Yb compounds starts to increase with rising pressure,²⁷ since the atomic radius of the $4f^{13}$ state is smaller than that of the $4f^{14}$ one. n_f is related to T_K via

$$n_f/(1-n_f) = N_f \Delta / T_K, \quad (3)$$

where $\Delta = \pi |V_{kf}|^2 N(E_F)$ is the hybridization strength between $4f^{14}(ds)^2$ and $4f^{13}(ds)^3$ electronic states, and N_f represents the degeneracy of the f electrons.²⁸ Hence, if n_f increases, $N_f \Delta / T_K$ increases as a whole. Pressure, however, influences both the hybridization parameter $N_f \Delta$ as well as the Kondo temperature T_K . Since T_K changes exponentially [$T_K = D \exp(-\pi |\epsilon_f| / N_f \Delta)$, D is the effective band width], it varies more rapidly than the hybridization parameter. We, therefore, expect that the Kondo temperature decreases upon pressure as the number of f holes increases.

A decrease of T_K , however, can also be obtained from a change of the hybridization with pressure, which does not necessarily require a change in the f hole count.

The pressure response of $T_{\rho,low}^{\max} \propto T_K$ (Ref. 8) allows the determination of the electronic Grüneisen parameter of this series according to

$$\Gamma_e = -\partial \ln T_K / \partial \ln V = B \partial \ln T_K / \partial p, \quad (4)$$

where B is the bulk modulus of the system.¹⁴ Γ_e is evaluated as -102 , -152 , and -90 for $x = 1.3$, 1.4 , and 1.5 , respectively, if B is assumed to be 1 Mbar. The latter value is considered to be typical for Yb systems.²⁹ Values of Γ_e deduced according to Eq. (4) are substantially larger than Γ_e of simple metals but match that of typical highly correlated electron systems such as CeCu_6 [$\Gamma_e = 57$ (Ref. 30)] or YbCuAl [$\Gamma_e = -87$ (Ref. 31)]. The negative value of Γ_e obviously indicates that $\partial T_K / \partial p < 0$, again a typical feature of Yb compounds.

The concentration-dependent variation of Γ_e is likely a consequence of the proximity to the onset of long-range magnetic order as the Al content increases. Thus, it can be supposed that the alloy with $x = 1.4$ and $\Gamma_e = -152$ is nearest to that critical concentration, where the quantum-critical phase transition is expected. In fact, systems which have been studied in great detail like Ce_7Ni_3 (Ref. 32) exhibit also dramatic variations of Γ_e . At pressures next to the critical

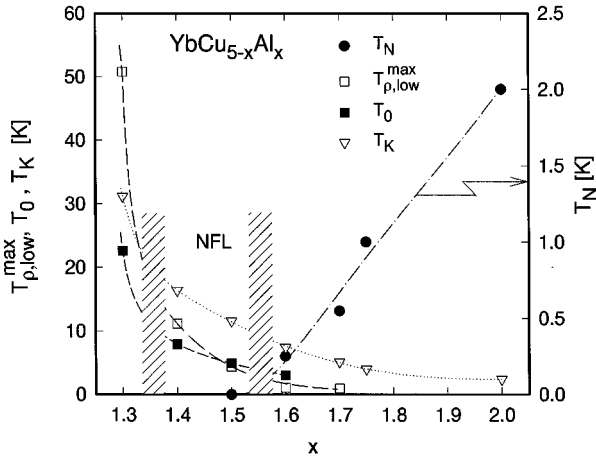


FIG. 12. Concentration dependence of characteristic temperatures of $\text{YbCu}_{5-x}\text{Al}_x$; $T_{\rho,low}^{\max}$ is the low-temperature maximum of the electrical resistivity, T_0 is the scaling temperature according to Eq. (1). The antiferromagnetic ordering temperature T_N for $x=1.6$ and $x=1.7$ as well as T_K are taken from Ref. 5. The concentration range between the hatched areas is the approximate extension of the NFL.

pressure p_c where NFL behavior occurs, $\Gamma_e = 220$, while well below and above p_c the Grüneisen parameter substantially decreases.³² A similar evolution of the Grüneisen parameter can be deduced for $\text{Ce}(\text{Cu},\text{Au})_6$.³³ The alloy $\text{CeCu}_{5.8}\text{Au}_{0.2}$ with long-range magnetic order at $T_N(p=1 \text{ bar}) \approx 0.24 \text{ K}$ —next to the critical concentration $\text{CeCu}_{5.9}\text{Au}_{0.1}$ —is characterized by $\Gamma_e \approx 280$ while Γ_e is already reduced to about 105 for $\text{CeCu}_{5.7}\text{Au}_{0.3}$, which exhibits more stable moments. On the other side, CeCu_6 , with a Fermi-liquid ground state, exhibits $\Gamma_e \approx 57$.³⁰

An interesting feature is evident from the field-dependent variation of $T_{\rho,low}^{\max}$. As shown in Fig. 11(b), this quantity grows almost linearly with rising fields. Such a behavior, most likely, may be understood from the general behavior of the characteristic temperature scale T_K as a function of the external magnetic fields. In the scope of the Bethe-ansatz solution of the Anderson Hamiltonian, Rajan³⁴ has shown that, e.g., the maximum of the specific heat, which is directly related with T_K , shifts to higher temperatures. Such a behavior may be considered to occur formally from a growing value of T_K . In the very simple $j=1/2$ picture of the Kondo effect, the external field causes a splitting of a magnetic triplet state above the nonmagnetic singlet ground state, thus an occupation of levels at higher energies is invoked and the specific heat maximum moves to higher temperatures. Similarly, the field variation of $T_{\rho,low}^{\max}$ may be accounted for. In an attempt to describe the effect of the magnetic field on $T_{\rho,low}^{\max}$ more quantitatively, we considered the variational approach of the impurity Kondo problem.²⁸ In the variational calculation, the Kondo temperature T_K , which according to Cox and Grewe⁸ can be identified in zero fields with $T_{\rho,low}^{\max}$, is the energy separation between the Kondo singlet ground state and the $4f$ orbital, the latter being in our case the CF ground state. An external magnetic field causes a Zeeman splitting of this level and concomitantly, the energy of the Kondo singlet lowers. The mean energy distance \bar{T}_0 between the Kondo singlet and the Zeeman split ground CF state there-

fore increases, and we can identify $\bar{T}_0(B)$ with $T_{\rho,low}^{\max}(B)$. The results of the variational calculation of the field dependence of $\bar{T}_0(B)$ are shown in Fig. 11(b) as solid lines, assuming $\bar{T}_0(B \rightarrow 0) = 50, 12,$ and 4 K for $x = 1.3, 1.4,$ and 1.5 , respectively, and the field applied along the c axis. Reasonable agreement is found between the experimental data and the theoretical predictions in spite of the crudeness of the model. The calculated curves are characterized by $\bar{T}_0(B) \propto B^2$ for low fields, while $\bar{T}_0(B) \propto B$ in the high-field limit.

Most of the experimental findings on $\text{YbCu}_{5-x}\text{Al}_x$ indicate that the significant deviations of the physical properties from a FL behavior for alloys near to the critical concentration ($x_{\text{cr}} \approx 1.5$) may descend from the evolution of long-range magnetic order for $x > x_{\text{cr}}$. Thus, a quantum-critical phase transition is expected at x_{cr} . Many of the yet studied NFL systems are explained in terms of such a phase transition at $T=0$. Enhanced spin fluctuations in these systems are supposed to cause the breakdown of a Fermi-liquid ground state. The latter, as it is well known, occurs only in the case of weak interactions.

Another route to obtain NFL, stressed in literature,³⁵ is a distribution of local Kondo temperatures due to disorder in the investigated system. This can cause a broad distribution of local energy scales with arbitrarily small values of T_K . Hence, the magnetic moments at certain sites of the lattice are unquenched at low temperatures and dominate thermodynamic and transport properties.³⁵ The presence of such unquenched moments leads then to the formation of a non-Fermi-liquid phase. $\text{UCu}_{5-x}\text{Pd}_x$ is considered as the best example, where a NFL behavior results from disorder due to the random substitution of Cu/Pd.³⁶ Different from the present Yb series, $\text{UCu}_{5-x}\text{Pd}_x$ crystallizes in the cubic AuBe_5 structure. Strong disorder as the central idea of the above model causes usually that $\rho(T)$ of such alloys do not enter a coherent state at low temperatures as reflected from a substantial decrease of the resistivity on lowering the temperature. Rather, $\rho(T)$ increases steadily with decreasing temperatures, similarly to single impurity Kondo systems. In fact, such a $\rho(T)$ dependence was reported for $\text{UCu}_{5-x}\text{Pd}_x$.^{36,37} The particular resistivity behavior of $\text{YbCu}_{5-x}\text{Al}_x$ for concentrations $1.7 \leq x \leq 1.3$ hints, however, to the evolution of a probably not fully developed coherent state at low temperatures. Support for such a conclusion is revealed from particular features in the energy-dependent optical conductivity $\sigma(\omega)$.²⁶ While for samples $x < 1.5$ the optical conductivity shows a well-defined structure at lowest frequencies, associated with a plasma resonance, this typical sign of a coherent ground state vanishes progressively for $x \geq 1.5$ and becomes reminiscent of incoherent, single impurity Kondo systems.

A tentative phase diagram for this series is depicted in Fig. 12, tracing the general trends of $\text{YbCu}_{5-x}\text{Al}_x$. When the Al concentration increases, the hybridization and thus T_K becomes lower, enabling long-range magnetic order beyond a critical concentration $x_{\text{cr}} \approx 1.5$.

V. SUMMARY

Measurements of thermodynamic quantities like specific heat and of the pressure and field-dependent resistivity of

$\text{YbCu}_{5-x}\text{Al}_x$ reveal substantial deviations from a Fermi-liquid behavior for Al concentrations near to $x \approx 1.5$. This is concluded from a nonquadratic low-temperature behavior of the electrical resistivity as well as from the negative logarithmic contribution to the temperature-dependent specific heat. Moreover, the Grüneisen parameter Γ_e of alloys near to $x \approx 1.5$ is extraordinarily large and of comparable magnitude to other NFL systems near to their respective quantum critical point.

The most likely mechanism for the observed NFL behavior is the proximity of the samples with $1.3 < x < 1.6$ to that Al content, where long-range magnetic order sets in ($x \approx 1.6$). In the vicinity of a magnetic instability at $T=0$, strong spin fluctuations at finite temperatures occur, leading to deviations of the electrical resistivity from the T^2 behavior and to the appearance of a $-\ln(T)$ dependence in the specific heat. However, both magnetoresistance and preliminary optical conductivity data indicate that for sufficiently large values of Al the system gradually loses coherence, too.

The reason for the crossover of the system from a non-magnetic ground state for $x < 1.6$ to a state with long-range

magnetic order for $x \geq 1.6$ is assumed to be caused by the growing valency of the Yb ion in $\text{YbCu}_{5-x}\text{Al}_x$ due to the Al/Cu substitution. Concomitant with the increase of the valency is a decrease of the Kondo temperature of the series. The latter observation follows in a similar manner from the Mössbauer measurements,⁵ from the low-temperature specific heat and from the low-temperature maxima of the electrical resistivity as well. Due to the substantial lowering of T_K , both crystal-field splitting and RKKY interactions become comparable and eventually exceed T_K . The former effect causes that the degeneracy of the ground state declines, thus, favoring a magnetically ordered state,³⁸ in line with $T_{\text{RKKY}} > T_K$ upon the growing Al concentration.

ACKNOWLEDGMENTS

This work was supported by the Austrian Science Foundation Projects No. P 10947 and P 12899, and by Conicet (Res. No. 811). One of us (A.G.) is grateful to the ESF (project FERLIN) for financial support.

-
- ¹E. Bauer, R. Hauser, E. Gratz, D. Gignoux, D. Schmitt, and J.G. Sereni, *J. Phys.: Condens. Matter* **4**, 7829 (1992); E. Bauer, K. Payer, R. Hauser, E. Gratz, D. Gignoux, D. Schmitt, N. Pillmayr, and G. Schaudy, *J. Magn. Magn. Mater.* **104-107**, 651 (1992).
- ²E. Bauer, R. Hauser, L. Keller, P. Fischer, O. Trovarelli, J.G. Sereni, J.J. Rieger, and G.R. Stewart, *Phys. Rev. B* **56**, 711 (1997).
- ³J.A. Hertz, *Phys. Rev. B* **14**, 1165 (1976).
- ⁴T. Moriya and T. Takimoto, *J. Phys. Soc. Jpn.* **64**, 960 (1995).
- ⁵P. Bonville, E. Vincent, and E. Bauer, *Euro. Phys. J B B* **8**, 363 (1999).
- ⁶E. Bauer, M. Rotter, L. Keller, P. Fischer, M. Ellerby, and K. McEwen, *J. Phys.: Condens. Matter* **6**, 5533 (1994).
- ⁷A. Eiling and J. Schilling, *J. Phys. F* **11**, 623 (1981).
- ⁸D. Cox and N. Grewe, *Z. Phys. B* **71**, 321 (1988).
- ⁹D. Cornut and B. Coqblin, *Phys. Rev. B* **5**, 4541 (1972).
- ¹⁰P. Bonville and E. Bauer, *J. Phys.: Condens. Matter* **8**, 7797 (1996).
- ¹¹A.C. Hewson, *The Kondo Problem to Heavy Fermions*, Cambridge Studies in Magnetism, Vol. 2 (Cambridge University Press, Cambridge, 1993).
- ¹²A. Iandelli and A. Palenzona, *J. Less-Common Met.* **25**, 333 (1971).
- ¹³B. Bogenberger and H. von Löhneysen, *Phys. Rev. Lett.* **74**, 1016 (1995) and references cited therein.
- ¹⁴J.D. Thompson, in *Frontiers in Solid State Sciences, Vol. 2*, edited L.C. Gupta and M.S. Multani (World Scientific, London, 1993), p. 107.
- ¹⁵H. Kaga and H. Kubo, *Physica B* **147**, 147 (1987).
- ¹⁶H. Kaga, H. Kubo, and T. Fujiwara, *Phys. Rev. B* **37**, 341 (1988).
- ¹⁷S. Doniach, *Physica B* **91**, 231 (1977).
- ¹⁸A.M. Tselvelik and M. Reizer, *Phys. Rev. B* **48**, 9887 (1993).
- ¹⁹M.A. Continentino, *Z. Phys. B* **101**, 197 (1996).
- ²⁰A.J. Millis, *Phys. Rev. B* **48**, 7183 (1993).
- ²¹J.G. Sereni, C. Geibel, M.G. Berisso, P. Hellmann, O. Trovarelli, and F. Steglich, *Physica B* **230-232**, 580 (1997).
- ²²G.G. Lonzarich (unpublished).
- ²³F. Steglich, B. Buschinger, P. Gegenwart, M. Lohmann, R. Heflerich, C. Langhammer, P. Hellmann, L. Donnevert, S. Thomas, A. Link, C. Geibel, M. Lang, G. Sparn, and W. Assmus, *J. Phys.: Condens. Matter* **8**, 9909 (1996).
- ²⁴J. Sereni, *J. Phys. Soc. Jpn.* **67**, 2901 (1998).
- ²⁵C.J. Pethick and D. Pines, in *Recent Progress in Many-Body Theories*, edited by A.J. Kallio, E. Pajanne, and R.F. Bishop (Plenum, New York, 1988), p. 17.
- ²⁶M. Galli, E. Bauer, and F. Marabelli (unpublished).
- ²⁷D. Wohlleben, in *Moment Formation in Solids*, edited by W.J.L. Buyers (Plenum, New York, 1984), p. 171.
- ²⁸O. Gunnarsson and K. Schönhammer, *Phys. Rev. B* **28**, 4315 (1983).
- ²⁹E. Bauer, R. Hauser, E. Gratz, K. Payer, G. Oomi, and T. Kagayama, *Phys. Rev. B* **48**, 15873 (1993); E. Bauer, E. Gratz, R. Hauser, A. Galatanu, A. Kottar, H. Michor, W. Perthold, T. Kagayama, G. Oomi, N. Ichimiya, and S. Endo, *ibid.* **50**, 9300 (1994).
- ³⁰A. deVisser, J.J.M. Franse, and J. Flouquet, *Physica B* **161**, 311 (1989).
- ³¹A. Bleckwedel and A. Eichler, in *Physics of Solids Under High Pressure*, edited by J.S. Schilling and R.N. Shelton (North-Holland, Amsterdam, 1981) p. 323.
- ³²K. Uemo, H. Kadomatsu, and T. Takabatake, *J. Phys.: Condens. Matter* **8**, 9743 (1996).
- ³³H. von Löhneysen, *J. Phys.: Condens. Matter* **8**, 9689 (1996).
- ³⁴V.T. Rajan, *Phys. Rev. Lett.* **51**, 308 (1983).
- ³⁵E. Miranda, V. Dobrosavljevic, and G. Kotliar, *J. Phys.: Condens. Matter* **8**, 9871 (1996).
- ³⁶B. Andraka and G.R. Stewart, *Phys. Rev. B* **47**, 3208 (1993).
- ³⁷R. Chou, S.H. Han, M.B. Maple, M.C. Aronson, and H. von Löhneysen, *Physica B* **230-232**, 600 (1997).
- ³⁸P. Coleman, *Phys. Rev. B* **29**, 3035 (1984).